Optik - International Journal for Light and Electron Optics 212 (2020) 164712

Contents lists available at ScienceDirect

Optik

journal homepage: www.elsevier.com/locate/ijleo

Original research article

Preparation and characteristics of SnS_2 saturable absorber and its application in passively Q-switched Nd:YAG/Cr^{4+}:YAG laser

Rui Wang[a,b,*], Luwei Zhang[a,b], Tao Sun[a,b], Hualong Wang[a,b]

[a] Changchun Institute of Optics, Fine Mechanics and Physics, Chinese Academy of Sciences, Changchun 130033, China

[b] State Key Laboratory of Laser Interaction with Matter, Changchun Institute of Optics, Fine Mechanics and Physics, Chinese Academy of Sciences, Changchun 130033, China

ARTICLE INFO

Keywords:
SnS_2 saturable absorber
Nd:YAG/Cr^{4+}YAG
Passively Q-switched

ABSTRACT

In this paper, the preparation and characteristics of SnS_2 saturable absorber were demonstrated, and the SnS_2 saturable absorber was used in Nd:YAG/Cr^{4+}:YAG laser. Under different output coupler, repetition rate showed the range from 1.5 kHz to 6.2 kHz and pulse width showed the range from 3.1 ns to 5.8 ns with the increasing pump power. The max pulse energy was 29 μJ with peak power of 9.4 kW.

1. Introduction

Passively Q-switched (PQS) operation provides lower output performances compared to active Q-switched (AQS), but it shows more advantages like simple cavity structure, lower costs and reliability. The PQS technique, generated laser pulse width less than microsecond, is of great significance for scientific research, military applications, materials processing, medical examination and remote sensing [1–4]. In PQS lasers, the saturable absorbers (SAs) are recognized as the key device. In recent decades, the SAs had experienced a long process of development. For example: dyes, crystals such as Cr^{4+}:YAG [5], Cr^{2+}:ZnSe [6,7], SESAM/SBR-based nonlinear mirrors [8,9] and graphene or graphene-like materials. Among these saturable absorber (SA) materials, Cr^{4+}:YAG crystals, with excellent heat conductivity, stable optical property and heat conductivity, have been employed for LD-pumped composite crystal lasers [10,11]. Generally, Cr^{4+}:YAG laser could not generate high peak power pulses.

In order to develop highly compact laser system, we combined the gain medium and the SA. Nd:YAG/Cr^{4+}:YAG composite crystal with thin pieces of Nd:YAG bonded to thin pieces of Cr^{4+}:YAG by using diffusion composite technique, is widely used to fabricate micro compact PQS lasers with infrared output [12]. On one hand, compared to the co-doped Nd:YAG laser media and the Cr^{4+}:YAG single crystal lasers, composite crystals have the advantages such as rather slight thermal effects of active medium and compact laser cavity [13]. On the other hand, with the same Cr^{4+}:YAG crystal and cavity, the pulse width in Nd:YAG/Cr^{4+}:YAG composite crystal exhibited shorter [13,14]. Therefore, the composite crystal could be recognized as an ideal laser material with some advantages such as: low thermal lens effect by the end face deformation, high light-to-light conversion efficiency and damage threshold, good output beam quality and compact laser cavity.

Among the transition metal sulfides (TMDs) layered materials, SnS_2 exhibits excellent photoelectric properties such as deeper modulation depth than graphene and wider modulation wavelength range than MoS_2 and WS_2 [15–22]. These properties make SnS_2 a good candidate as the SA in lasers, but there are still few reports about the SnS_2 SA used in composite crystal lasers. In order to obtain shorter pulse width and highly stable PQS operation, the SnS_2 SA and the Nd:YAG/Cr^{4+}:YAG composite crystal were combined in

* Corresponding author at: Changchun Institute of Optics, Fine Mechanics and Physics, Chinese Academy of Sciences, Changchun 130033, China.
E-mail address: darui99999@163.com (R. Wang).

https://doi.org/10.1016/j.ijleo.2020.164712
Received 18 February 2020; Accepted 7 April 2020
0030-4026/

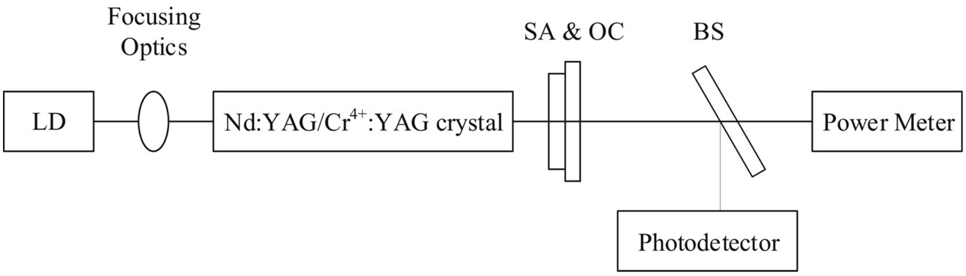

Fig. 1. Experimental setup of the PQS Nd:YAG/Cr^{4+}:YAG laser.

laser cavity.

In this paper, the preparation and characteristics of SnS_2 SA were demonstrated, and the SnS_2 SA was used in PQS Nd:YAG/Cr^{4+}:YAG laser. Typical pulse profile and beam profile of the PQS Nd:YAG/Cr^{4+}:YAG laser were also demonstrated. Moreover, the SnS_2 SA-based solid-state laser is reported for the first time [23,24].

2. Experimental setup

The experimental setup of the PQS Nd:YAG/Cr^{4+}:YAG laser was shown in Fig. 1. The central wavelength of fiber-coupled laser diode was 808 nm, and the max output power was 3 W. The beam spot radius was 200 μm with numerical aperture of 0.22. The cavity length of 14 mm was designed. The input side was a 1.1 % doped Nd:YAG with the dimensions of 3 × 3 × 5 mm^3, and the other side was a 3 × 3 × 2 mm^3 Cr^{4+}:YAG crystal with an initial transmission of 65 %. The crystal was HT-coated at 808 nm and HR-coated at 1064 nm on input side, and AR-coated at 1064 nm on the other side. The SnS_2 SA was employed. The composite crystal was cooled by TEC at the temperature of 28 °C. The output couplers (OCs) were flat mirrors with 1.5 %, 3%, 10 % and 27 % transmission at 1.06 μm. The temporal pulse profile was recorded by a digital oscilloscope (Agilent DSO7012B) and an InGaAs photodetector (Thorlabs PDA015C). The output power was measured by a power meter (Thorlabs PM100D).

3. Experimental results and discussions

3.1. Preparation and characterization of SnS_2 SA

The fabricating method of SnS_2 SA was liquid-phase stripping and demonstrated as follows: At first, 0.1 g of SnS_2 powder with diameter less than 10 μm was added into 25 ml analytical pure alcohol. Next, the solution was put in an ultrasonic machine for 10 h. After that, stirred the solution for 20 min with rotation rate of 1000 rpm. Then, got the supernatant liquid and dropped it on K9 substrate. Finally, left the substrate at 23℃ for half a day.

The characterization of SnS_2 SA was demonstrated in Fig. 2. As shown in Fig. 2(a) and (b), SnS_2 SA showed a broad transmission range from 700 nm to 1100 nm. The linear transmission and linear absorption coefficient at 1064 nm are 83.8 % and 0.0767, respectively.

The nonlinear absorption property of the SnS_2 SA was demonstrated in Fig. 2(c). The femtosecond laser with 150 fs pulse width, central wavelength at 1040 nm and the repetition rate of 32 MHz was used. The saturation intensity was 153.2 MW/cm^2 and the modulation depth was 7.9 %. In Fig. 2(d), Raman spectroscopy of the SnS_2 SA was shown. Two typical peaks at 205 cm^{-1} and 314 cm^{-1} are related to the E_g and A_{1g}^{1} vibrational modes. The AFM photograph and SEM photograph were shown in Fig. 2(e) and (f), the diameter and thickness of the SnS_2 SA were 300 nm and 5.72 nm (5 layers), respectively.

3.2. PQS Nd:YAG/Cr^{4+}:YAG laser

The stable PQS Nd:YAG/Cr^{4+}:YAG laser with SnS_2 SA was observed, and OCs with transmission of T = 1.5 %, 3%, 10 % and 27 % at 1064 nm were used.

Fig. 3 showed the relationship between output power and pump power at different output coupler (OC). With the increasing OC from 1.5% to 27%, the threshold pump power increased from 2.08 W to 2.22 W. Under pump power of 2.58 W: with the increasing OC from 1.5% to 27%, the output power increased from 22 mW to 180 mW, and the optical conversion efficiency increased from 0.85 % to 6.98 %.

Fig. 4 showed the variation of pulse width (PW) and repetition rate (RR) with increasing pump power at different OC. Under pump power of 2.58 W: with the increasing OC from 1.5% to 27%, the PW decreased from 4.4 ns to 3.1 ns, and the RR increased from 4.9 kHz to 6.2 kHz. Under pump power of 2.58 W and 27 % OC, the maximum pulse energy of 29 μJ with highest peak power of 9.4 kW was obtained.

Fig. 5 showed the pulse profile and beam profile of the PQS operation with 27 % OC. The far-field beam profile was shown in Fig.6(c), and the 808 nm pump laser oscillates at the fundamental transverse mode.

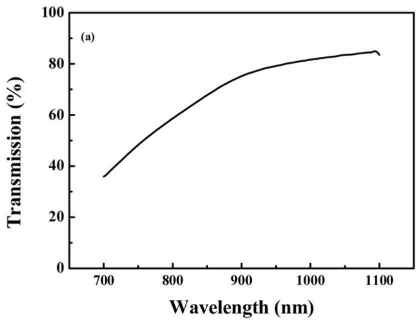

(a) linear transmission spectrum

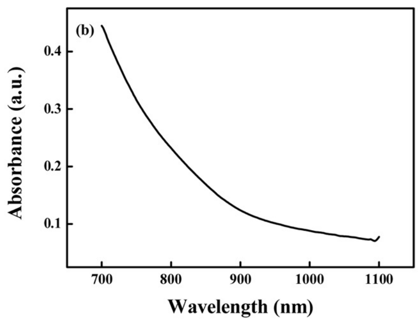

(b) linear absorption spectrum

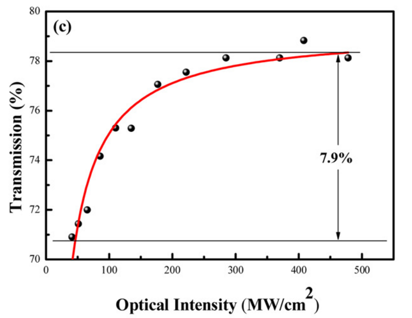

(c) nonlinear absorption spectrum

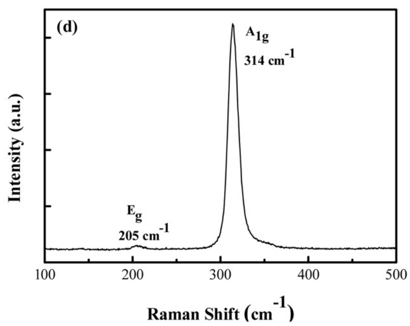

(d) Raman spectrum

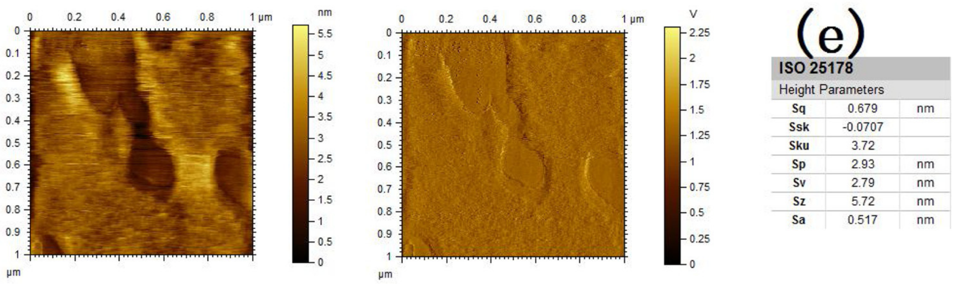

(e) AFM photograph

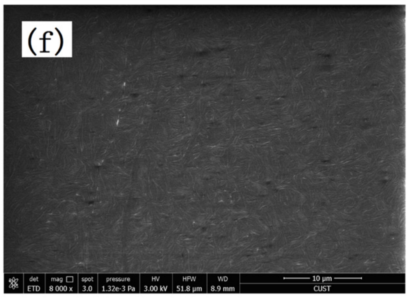

(f) SEM photograph

Fig. 2. Characterization of SnS_2 SA.

4. Conclusion

Based on the preparation and characteristics of the SnS_2 SA, a compact PQS Nd:YAG/Cr^{4+}:YAG laser have been demonstrated. With pump power of 2.58 W and 27 % OC: the output power was 180 mW with optical-optical conversion efficiency of 6.98 %, the

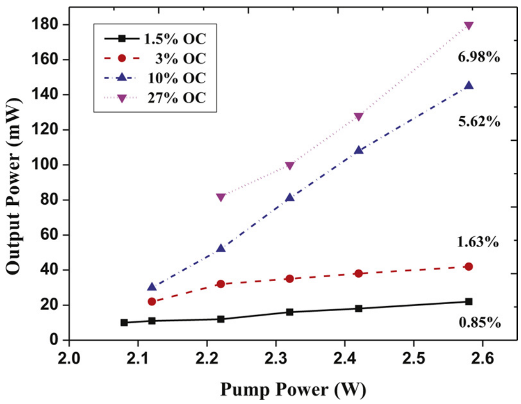

Fig. 3. Relationship between output power and pump power at different output coupler.

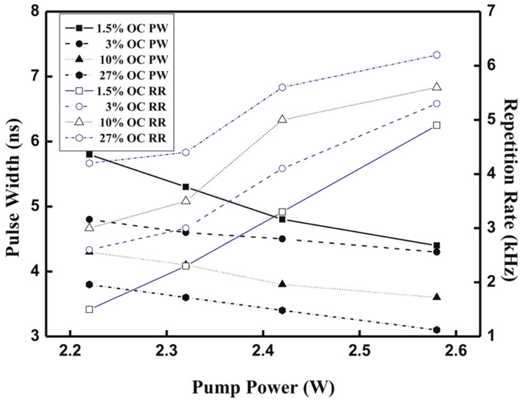

Fig. 4. Variation of pulse width and repetition rate with increasing pump power at different OC.

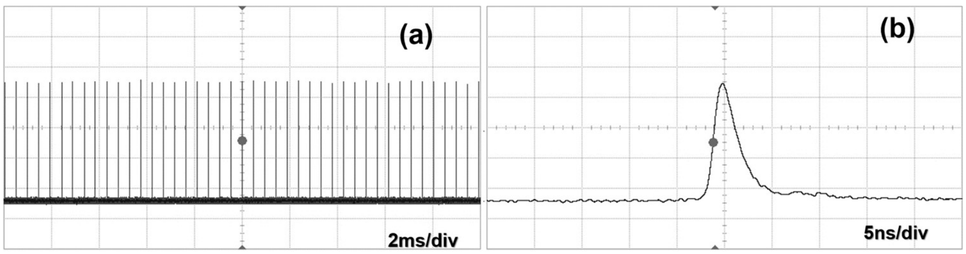

(a) Pulse trains (b) Typical pulse profile

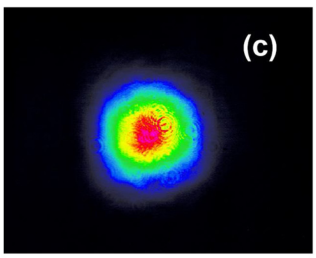

(c) typical beam profile

Fig. 5. Pulse profile and beam profile of the PQS operation with 27 % OC.

PW was 3.1 ns with RR of 6.2 kHz, and the single pulse energy of 29 μJ with peak power of 9.4 kW.

Funding

This work is supported by the Jilin Scientific and Technological Department Program (Grant No. 20190302050GX).

Declaration of Competing Interest

The authors declare no conflict of interest.

References

[1] Q. Song, G.J. Wang, B.Y. Zhang, W.J. Wang, M.H. Wang, Q.L. Zhang, G.H. Sun, Y. Bo, Q.J. Peng, Diode-pumped passively dual-wavelength Q-switched Nd:GYSGG laser using graphene oxide as the saturable absorber, Appl. Opt. 54 (10) (2015) 2688–2692.

[2] M.X. Li, G.Y. Jin, Y. Li, Diode-pumped passively Q-switched Nd:$GdTaO_4$ laser based on tungsten disulfide nanosheets saturable absorber at 1066nm, Infrared Phys. Technol. 90 (2018) 195–198.

[3] X. Zhao, Y. Li, H. Zhang, M.X. Li, Polarization sensitive ReS_2-GaSe nanosheets for Er&Yb co-doped fiber laser, Infrared Phys. Technol. 94 (2018) 219–222.

[4] Y. Li, X. Zhao, H. Zhang, M.X. Li, GaSe saturable absorber for mode-locked Er-doped fiber laser, Infrared Phys. Technol. 96 (2019) 325–329.

[5] A. Sennaroglu, Broadly tunable Cr^{4+}-doped solid-state lasers in the near infrared and visible, Prog. Quantum Electron. 26 (6) (2002) 287–352.

[6] A.V. Podlipensky, V.G. Shcherbitsky, N.V. Kuleshov, V.P. Mikhailov, V.I. Levchenko, V.N. Yakimovich, Cr^{2+}:ZnSe and Co^{2+}:ZnSe saturable-absorber Q switches for 1.54-μm Er:glass lasers, Opt. Lett. 24 (14) (1999) 960–962.

[7] H. Cankaya, U. Demirbas, A.K. Erdamar, A. Sennaroglu, Absorption saturation analysis of Cr^{2+}:ZnSe and Fe^{2+}:ZnSe, J. Opt. Soc. Am. B 25 (5) (2008) 794–800.

[8] U. Keller, K.J. Weingarten, F.X. Kärtner, D. Kopf, B. Braun, I.D. Jung, R. Fluck, C. Honninger, N. Matuschek, J.A. derAu, Semiconductor saturable absorber mirrors (SESAM's) for femtosecond to nanosecond pulse generation in solid-state lasers, IEEE J. Sel. Top. Quantum Electron. 2 (3) (1996) 435–453.

[9] S. Tsuda, W.H. Knox, S.T. Cundiff, W.Y. Jan, J.E. Cunningham, Mode-locking ultrafast solid-state lasers with saturable Bragg reflectors, IEEE J. Sel. Top. Quantum Electron. 2 (3) (1996) 454–464.

[10] J. Dong, P.Z. Deng, Y.P. Liu, Y.H. Zhang, J. Xu, W. Chen, X.L. Xie, Passively Q-switched Yb:YAG laser with Cr^{4+}:YAG as the saturable absorber, Appl. Opt. 40 (24) (2001) 4303–4307.

[11] J.J. Zheng, S.Z. Zhao, L. Chen, Laser-diode end-pumped passively Q-switched Nd:YVO_4 laser with Cr^{4+}:YAG saturable absorber, Opt. Eng. 41 (09) (2002) 2271–2275.

[12] G. Salamu, A. Ionescu, C.A. Brandus, O. Sandu, N. Pavel, T. Dascalu, High-peak power, passively Q-switched, composite, all-poly-crystalline ceramics Nd:YAG/Cr^{4+}:YAG laser and generation of 532-nm green light, Laser Phys. 22 (1) (2012) 68–73.

[13] X.Q. Yang, H.X. Wang, J.L. He, B.T. Zhang, H.T. Huang, A compact passively Q-switched intra-cavity frequency doubled Nd:YAG/Cr^{4+}:YAG composite crystal green laser, Laser Phys. 19 (10) (2009) 1964.

[14] Q. Song, G.J. Wang, B.Y. Zhang, S.H. Li, X.X. Gao, Y.L. Liu, W.J. Wang, Compact high stable passively Q-switched Nd:YVO_4 laser with Cr^{4+}:YAG, Optik 126 (20) (2015) 2442–2444.

[15] Q. Song, B.Y. Zhang, G.J. Wang, Characterization of $SnSe_2$ saturable absorber by THz-TDS and used in dual-wavelength passively Q-switched laser, Optik 174 (2018) 35–39.

[16] Q. Song, Z.Y. Wu, P.F. Ma, G.J. Wang, B.Y. Zhang, TiS_2, MoS_2, WS_2/Sb_2Te_3 mixed nanosheets saturable absorber for dual-wavelength passively Q-switched Nd:GYSGG Lase, Infrared Phys. Technol. 92 (2018) 1–5.

[17] Q. Song, B.Y. Zhang, G.J. Wang, THz absorption spectrum employed for characterize the mixed Gallium selenide-Tin disulfide saturable absorber and its application for passively Q-switched solid state laser, Infrared Phys. Technol. 93 (2018) 87–90.

[18] M.X. Li, Y. Li, X.L. Qin, Y. Tan, Ultrafast absorption of $SnSe_2$-MoS_2 heterojunction nanosheets and its application in passively Q-switched Nd:GGG laser, Optik 189 (2019) 9–14.

[19] H.R. Yang, X.M. Liu, Nonlinear optical response and applications of tin disulfide in the near-and mid-infrared, Appl. Phys. Lett. 110 (17) (2017) 171106.

[20] J. Li, Y.F. Zhao, Q.Y. Chen, K.D. Niu, R.Y. Sun, H.N. Zhang, Passively mode-locked ytterbium-doped fiber laser based on SnS_2 as saturable absorber, IEEE Photonics J. 9 (6) (2017) 1–7.

[21] G.Q. Li, C. Wu, S.Y. Zhang, J. Su, T. Li, Passively Q-switched Er:YAG laser at 1645 nm with SnS_2 as a novel saturable absorber, Optik 183 (2019) 163–167.

[22] X.J. Dong, Z.Q. Li, C. Pang, N.N. Dong, H.L. Jiang, J. Wang, F. Chen, Q-switched mode-locked Nd:GGG waveguide laser with tin disulfide as saturable absorber, Opt. Mater. 100 (2020) 109702.

[23] K.D. Niu, R.Y. Sun, Q.Y. Chen, B.Y. Man, H.N. Zhang, Passively mode-locked Er-doped fiber laser based on SnS2 nanosheets as a saturable absorber, Photonics Res. 6 (2) (2018) 72–76.

[24] K.D. Niu, Q.Y. Chen, R.Y. Sun, B.Y. Man, H.N. Zhang, Passively Q-switched erbium-doped fiber laser based on SnS_2 saturable absorber, Opt. Mater. Express 7 (11) (2017) 3934–3943.